

Performance curve fitting to the operating point of fans

Cheng-Hsing Hsu¹, Kuang-Yuan Kung^{2,*}, Ching-Chuan Chang¹, and Chia-Chuan Kuo¹

¹Department of Mechanical Engineering Chung-Yuan Christian University.

²Department of Mechanical Engineering Nanya Institute of Technology.

*414 Sec. 3 Chung Shang East R. Chung Li 320 TAIWAN, ROC

ky.kung@msa.hinet.net

<http://www.nanya.edu.tw>

Abstract: This paper explores utilization of reverse engineering for dimensionless analysis of the performance curve of the fan. Utilizing the function curve and data provided in the reference material, this paper identifies interactions among major parameters affecting the static pressure and flow of the fan. Following the fitting, the equation $P(X)$ is expressed via Chebyshev polynomial. It simplifies the performance curve of the fan to match the impedance curve of the system. The corresponding diagram obtained can be used to predict the operating point of dimensionless performance curve of the fan to match the impedance curve of the system. In comparison with the conventional approach, the operating point of the research method registers an error rate of under 4.97%. This method can help save the cost of experiment or simulation, accelerate the speed of operating point search and reduce the size of the fan databank.

Keywords: Chebyshev polynomial, dimensionless, impedance curve, operating point, reverse engineering, performance curve,

1. Introduction

The working principle of the fan mainly utilizes rotation to stir the air to remove the heat of a heating element and reduce the temperature. In general, when the design and profiling of a heating element is completed the impedance curve of the element is fixed. Therefore, changing the fan design in association with the cooling element in order to enhance the overall heat-dissipation efficiency is frequently employed in the design process for heat-dissipation element [1-4]. How to identify the performance curve of different fan, as a result, is an important issue in design of heat-dissipation element. The performance curve of the fan is mainly acquired via experiment and simulation. Though less costly, simulation is more time consuming, and there is discrepancy between its outcome and reality. The

two primary methods currently employed to determine the performance curve of the fan are known for their individual strengths and weaknesses. Therefore, we would like to find an approach that has the strengths of both and weaknesses of neither. This method must be with the following features:

1. Quickly determine the performance curve of the fan.
2. The performance curve obtained is close to reality.
3. Significantly help save cost.

Wind volume and wind pressure as important indicators for testing fan functions. Generally, there are two ways to test wind volume and wind pressure. The first uses the wind tunnel method, and the second uses the two bin system. For normal ventilation, we need to overcome the resistance of the aeration course of the fan. The fan must generate

a pressure that overpowers the ventilation resistance. The pressure change measured is called the static pressure, which is the difference between the maximum static pressure and atmospheric pressure. To attain the goal of ventilation, both static pressure and dynamic pressure are required. The greater the wind pressure, the higher the fan's ventilation ability is. In actual applications, the nominal maximum wind flow does not equal to the wind flow received by the cooling fins. According to Bernoulli's Law, the air's pressure decreases as its flow velocity increases. On its course of movement, the air flow will meet the resistance of the radiation sheets whose geometric shape will prevent the air from free flowing. Therefore, there has to be an optimal operational point, which is the intersection of the fan function curve and the wind resistance curve. At the optimal operation point, the fan function curve has the lowest slope, and the variation rate of the system property curve is minimum. At this moment, the fan has the best static efficiency (wind flow X wind pressure / power consumption). For reducing system resistance, we sometimes choose smaller fans, which can have the same wind pressure too

This study employs reverse engineering and utilizes dimensionless analysis in tandem with fitting curve analysis to engage heat-dissipation fans, which currently sells in the market, in simplified performance curve analysis. It discusses prediction of the performance curve of various rotating speed and the method for matching the corresponding systems [5-6]. It also determines the dimensionless static-pressure-flow equation. Inserting the various parameters for fan test, including current, voltage, rotating speed, external diameter of blade, hub diameter and noise, we can predict the operating point of dimensionless performance curve of the fan to match the impedance curve of the system and save the cost of experiment or simulation, accelerate

the speed of operating point search and reduce the size of the fan databank. This paper also explores the effect of parameters affecting the function curve of the fan, such as fan length, width, thickness, hub ratio (hub diameter/outer diameter), number of fins and rotation velocity, on the static pressure, flow and static pressure efficiency of the fan.

2. Research method

2.1 Data acquisition

The fan data used in this study comes from the performance curve of the AFB Series fans introduced by Delta Electronics Inc. in 2007 [7]. At least 60 points are obtained for a single performance curve as basis for fitting analysis.

2.2 Dimensionless analysis

Shown on the left side of Fig. 1(a) is the performance curve relationship diagram of AFB606020 Series fan from Delta Electronics Inc. [7]. CFM and mmH₂O represent air flow and static pressure respectively. Here the number 606020 indicates the length and width of the fan are 60mm each and the thickness is 20mm. From the diagram we learn that there is a performance curve corresponding to each rotating speed. There are five performance curves corresponding to the five rotating speeds. This study bases its analysis on dimensionless parameters. In its attempt to simplify the analysis into a single performance curve via the following combination:

$$P^* = \frac{P}{\rho \times D^2 \times n^2} \quad (1)$$

$$Q^* = \frac{Q^V}{Q_{\max}^V}, \text{ in which}$$

$$Q^V = \sqrt[3]{Re} \times \ln \sqrt{\frac{V \times I \times g}{\mu \times n^4 \times D^4 \times (dB - A)}} \quad (2)$$

$$\eta = \frac{P \times Q}{V \times I} \quad (3)$$

Following the curve fitting, it is discovered that the performance curves of the five rotating speeds are concentrated and can be represented by one dimensionless curve. The advantages of the method of this study include:

1. Only need to store one performance curve of the fan data and (at least) one set of maximum flow rate and maximum static pressure, as well as the corresponding rotating speed.
2. When the quantity of fan data increases, the size of the databank can be reduced.
3. Reduced data can accelerate operating point search.

2.3 Curve fitting

This study employs the Matlab software of The Math Works Inc.® to complete the fitting process. Afterwards, the equation $P(x)$ is expressed via Chebyshev polynomial.

$$P(x) = \frac{a_0}{2} + \sum_{i=1}^n a_i T_i(x), T_i(x) = \cos n\theta, \quad n=0,1,\dots, \quad a_i = \frac{2}{\pi} \int_{-1}^1 \frac{f(x)T_i(x)}{\sqrt{1-x^2}} dx \quad (4)$$

$$T_{n+1}(x) + T_{n-1}(x) = 2xT_n(x), \quad T_0(x) = 1, \quad T_1(x) = x \quad (5)$$

3. Results and discussion

The results of this study are discussed in the following paragraphs including data fitting result, fan and system matching, and fitting curve error analysis.

3.1 Data fitting result

In accordance with test data of fans of different sizes and rotating speeds, Fig. 1(a) and Fig. 2(a) shows the performance curves of different fans. The

data comes from [7] –the fans are AFB606020 and AFB353510 respectively. The fan performance curves for the reference data are drawn after data conversion. Following dimensionless fitting of equations (1) and (2), the diagrams are shown on Fig. 1 (b) and Fig. 2(b). The equivalent circular size is actually determined proportionally by measuring the outer size of the fan provided in the reference material. The parameter values of the voltage, current and noise are also obtained through the published data provided in the reference material [7]. The fitting identifies high similarity, indicating this study method can successfully determine a single performance curve via fitting. From Fig. 3 we find that the more obvious the stalling zone of the original performance curve, the more it passes the fitted x and the more items of the polynomial is need. In Fig. 3, when Q^* shifts from 0.75→0.88, the static pressure shows no significant changes. The stalling zone is a phenomenon of boundary layer separation. When the rotating speed of the fan reaches certain degree, the air will form this phenomenon on the surface of the blades. As this phenomenon worsens, stalling takes place. Table 1 shows the coefficient values of $T_i(x)$ after fitting of different fans. From Table 1 we find that the higher order of the $T_i(x)$, the higher the coefficient value will be with exclusion of the last term. There are two reasons causing different levels of fitting. The first is that when the original performance curves of different rotating speeds are similar, and the stalling zone is not obvious, the order of the post-fitting diagram is lower and the diagram is smoother. When the stalling zone of the original performance curve at different speed becomes obvious, the order of the post-fitting diagram will be higher and the diagram will show greater fluctuation. Second, when the distance between the diagrams of the original performance curves of different rotating

speeds is greater, or some of the curves show more drastic fluctuations, the order of the post-fitting diagram will be higher.

Physical meaning of the order of the fitting curve: Take Fig. 1, Fig. 2 and Fig. 3 for example. The number of blades of the fan is fixed at 7. Following the fitting, it is discovered that the stalling zone of the performance curve of higher rotating speed is more obvious, meaning the number of the order requiring fitting is higher. Conversely, the fitting curve of lower rotating speed is smoother and the order requiring fitting is lower. Thereby we learn that the rotating speed has impact on the fitting. Physical meaning of the coefficients of the fitting curve: From Table 1 we can see the parameter values of post-fitting $T(x)$ of different fans. Thereby we learn that when the $T(x)$ order is higher, the coefficient value will be higher and the less the parameter of the higher level is negligible because it only affects the fluctuation end points of the diagram. The point is that the fitting curve we need to be at the stalling zone which refers to different rotating speeds in order to identify the optimal operating point for impedance matching of the system. When a fan is matched with the heat sink, the optimal operating point is at the intersection of the performance curve of the fan and the impedance curve of the system.

3.2 Fan and system matching

To verifying the matching of the impedance curve and the operating point of the performance curve, we examine the system impedance curve of the heat sink. Through the conventional matching model, this incorporates the performance curve of AFB606020 fan of different rotating speeds with the heat sink as shown in Fig. 4. We can see that the intersection of the system impedance curve and the performance curve of the fan of different rotating

speeds will be the operating point of the system (namely, the volume of the flow rate that will pass through the heat sink under different rotating speed when the fan and the heat sink is combined together).

The dimensionless analysis is based on system impedance curves corresponding to the performance curve of each rotating speed. Therefore, we can obtain the dimensionless analysis of the fan operating point as shown in Fig. 5.

3.3 Fitting curve error analysis

From Fig. 4 and Fig. 5 one can find that the discrepancy of system impedance curves following dimensionless analysis is limited. This way, after locating an operating point one can determine the operating point of various rotating speed with less guessing steps than the traditional approach. It can help us save the overall resources of system program. Based on combination of the short fan, the pressure and flow rate of the operating point under each rotating speed, as well as dimensionless pressure and flow rate, are shown in Tables 2&3, thereby we learn that the error between this method and traditional approach is under 5%. In comparison with the rotating speed error of the fan itself, this is acceptable. For converting P^* and Q^* into P (mm-H₂O) and Q (CFM), let's see rotating speed 4800rpm for example:

From measurement of reference [7] we learn that the equivalent diameter of AFB606020 (D)=2.35mm=0.0235m, the rotating speed n =4800rpm=80rps, air density ρ =1.23kg/m³, voltage=12V, current=0.18A, noise=33 (dB-A), air dynamic viscosity μ (1μ = 1.8×10^{-5} N-sec/m²), air motion viscosity ν = 1.47×10^{-5} (m²/sec), Q_{\max} =0.56 m³/min

The dimensionless conversion formula turns P^* into P_2 as follows:

$$P^* = \frac{P}{\rho \times D^2 \times n^2}$$

$$5.728 = \frac{P_2 \times 9.8}{1.23 \times 0.235^2 \times 80^2}$$

We have $P_2 = 2.54 \text{ mm-H}_2\text{O}$ and

$$P(\%) = \frac{P_2 - P_1}{P_1} = \frac{2.54 - 2.421}{2.42} = 4.9\%$$

Turns Q^* into Q_2 as follows:

$$Q^V = \sqrt[3]{\text{Re}} \times \ln \sqrt{\frac{V \times I \times g}{\mu \times n^4 \times D^4 \times (dB - A)}}$$

$$\text{Re} = \frac{\rho V D}{\mu}, \text{ Since } Q = AV, \text{ so } \text{Re} = \frac{4Q}{v\pi D}$$

$$Q_{\max}^V = \sqrt[3]{\frac{4 \times 0.02831 \times 0.56}{1.47 \times 10^{-5} \times 3.1416 \times 0.0235 \times 60}} \times \ln \sqrt{\frac{12 \times 0.18 \times 9.8}{1.8 \times 10^{-5} \times 80^4 \times 0.0235^4 \times 33}} = 137.057$$

$$Q^* = \frac{Q^V}{Q_{\max}^V}$$

$$0.8261 = \left(\sqrt[3]{\frac{4 \times 0.02831 \times Q_2}{1.47 \times 10^{-5} \times 3.1416 \times 0.0235 \times 60}} \times \ln \sqrt{\frac{12 \times 0.18 \times 9.8}{1.8 \times 10^{-5} \times 80^4 \times 0.0235^4 \times 33}} \right) / 137.057$$

We have $Q_2 = 12.837 \text{ CFM}$ and

$$Q(\%) = \frac{Q_2 - Q_1}{Q_1} = \frac{12.837 - 12.32}{12.32} = 4.19\%$$

3.4 Impact of fan parameters on flow and static pressure

The various design parameters of the fan have significant influence on the overall static pressure and flow. These parameters condition each other, engaging each other in complicated relations. It is the job of fan sheet design researchers to continue to adjust the parameters and find a combination that best meets operational requirements.

3.4.1 Effect of different fan thickness on function curve and static pressure efficiency

a. As shown in Fig. 6, when the fan length, width, hub ratio (0.47), fins and rotation velocity remain the same and the thickness is changed, we find that the static pressure increases with the fan thickness when the flow is fixed, and that the flow increases with the fan thickness when the flow is fixed. From the descriptions above we learn that fan thickness is a key factor affecting the function curve. From the figure we also observe that the static pressure and flow curves of the fan with a thickness of 15mm and 20mm are almost identical in the stall zone. This explains one thing. When searching for the operational point in conjunction with the resistance curve, under the same condition we can achieve the same cooling effect by selecting the thinner 15mm fan, which occupies less space and helps us save material cost.

b. As shown in Fig. 7, η increases as the fan thickness increases. The thickness difference results in a about 8% difference between the maximum value of η among the three. From the figure we also find that the 15mm-thickness curve and the 20mm-thickness curve for an obvious wave trough between the first and second peaks. The drop of η is supposed to be caused by the stall zone in Fig. 6.

3.4.2 Effect of different hub ratio on function curve and static pressure efficiency

a. As shown in Fig. 8, when the fan length, width, thickness and number of fins (7 sheets) remain the same. In the figure the hub ratio (0.55) of the higher rotation velocity is compared with the hub ratio (0.46) of the lower rotation velocity. When the pressure is greater than 1.1mmH₂O and is set at a fixed value, the fan air flow of the greater hub ratio is higher than the fan air flow of the lower hub ratio. But when the pressure is less than 1.1mmH₂O, the outcome is the opposite, and the maximum flow of the lower hub ratio is greater than the maximum flow of the higher hub ratio. Yet when the flow is

lower than 11.8CFM, the opposite outcome is derived, and the maximum static pressure of the higher hub ratio is greater than the maximum static pressure of the lower hub ratio. The greater the hub ratio (the smaller the extension), the greater the resistance is, and the higher the static pressure. The hub diameter is mainly determined by the power of the fan unit. So in fan design we have to consider not only the electrical power but also its effect on the static pressure and flow.

b. From Fig. 8 we learn that the hub ratio will reduce the maximum flow and increase the static pressure. From Fig. 9 we know that increase in hub ratio will help enhance the static pressure. The difference in hub ratio can cause a 2% difference in the maximum η values of the two. Therefore, one has to consider whether the overall static pressure efficiency is enhanced in fan design.

3.4.3 Effect of different length-width ratio on function curve and static pressure efficiency

a. As shown in Fig. 10, when the fan thickness, rotation velocity, number of fins (7 sheets) and hub ratio (0.62) remain the same, we learn that as the length \times width of the fan increases, the static pressure and the flow are both greater. We need to take into account the resistance curve of the entire system in order to determine the size of the fan and not just consider the shell size of the fan. Only when one choose a fan size and rotation velocity with satisfactory cooling efficiency, then one can meet the space and cost requirements.

b. From comparison of η in Fig. 11 we find that when Q^* is fixed, the greater the length \times width ratio, the greater η is. The discrepancy in the length \times width ratio causes a 4% difference in the maximum η values of the two. The maximum η values of AFB404015 is only 2.4%, mainly because the test

data of the flow-pressure figure of the function curve is lower, which results in a drop in η

3.4.4 Effect of different fin number on function curve and static pressure efficiency

a. In Fig. 12 when the fan length, width, hub ratio (0.43) and rotation velocity remain the same, the number of fins is 7 for the fan with greater thickness and the number of fins is 5 for the other fan. From Fig. 6 we learn that when the fan thickness increases the flow also increases. Yet Fig. 12 shows different outcomes. When CFM is less than 19, and when the flow or static pressure is fixed, the static pressure and flow rises with the rise in fan thickness. When CFM is higher than 19, the outcome is the opposite. When the number of fins is greater, the static pressure is also greater because the resistance is higher.

b. From Fig. 13 we can see that the static pressure efficiency of the fan with more fins and greater thickness is higher. The discrepancy between the maximum η values of the two is about 2%. From the figure we also find the η does not have a significant trough, mainly because the stall zone of the function curve in Fig. 12 is not obvious.

3.4.5 Effect of different rotation velocity on head height and curve

In Fig.14, AFB 606020 fan is used to test different rotation velocity. From the figure we can see that when the flow remains the same, the higher the velocity, the higher the H (head height) will be.

3.4.6 Effect of different rotation velocity on static pressure efficiency and dimensionless flow

In Fig. 15, when Q^* remains the same, the higher the rotation velocity, the higher the η will be. Under

lower rotation velocity, difference in η is less significant. Yet as the rotation velocity picks up, we find that difference in η becomes greater.

4. Conclusions

This paper employs reverse engineering and utilizes dimensionless analysis to integrate several performance curves of the fan under different rotating speeds into one. This simplified fitting curve can be used for matching with system impedance. This study discovers that putting the impedance curve through proper dimensionless process and incorporating it with the curve fitting of the fan can effectively reduce time cost to search for the operating point and help predict the operating point of the dimensionless performance curve of the fan and the impedance curve of the system. It can save the cost of experiment or simulation, accelerate the speed of operating point search and reduce the size of the databank. There is a maximum error of 4.97% between the method of this research and other conventional approach. Yet after the fan's rotating tolerance is included for comprehensive consideration, we find that the search method of this study is still within the acceptable error range. Concerning the effect of various fan parameters on static pressure and flow, all the parameters are associated. So we cannot find an ideal value by changing just one parameter. Through the limited fan testing data, function curve and fan configuration figures provided in the reference material, we identify the interactions of the parameters, which may serve as references for fan designers. The effects of fan design parameters on the function curve are as follows:

a. When the fan length, width, hub ratio, fins and rotation velocity remain the same and the

thickness is changed, we find that the flow and the static pressure increase with the fan thickness, and the corresponding η is also greater.

- b. When the fan length, width and thickness remain the same and the hub ratio is changed, we find that the higher the hub ratio, the smaller the flow. Static pressure: Since the resistance increases with the hub ratio, the static pressure is enhanced and the corresponding η is also greater.
- c. When the fan length and width are different and its thickness, rotation velocity, number of fins and hub ratio remain the same, the greater the fan length-width ratio, the greater the static pressure and flow become, and the greater the corresponding η .
- d. When the fan length, width, rotation velocity and hub ratio remain the same, and the thickness and number of fins are different, we find that the flow is greater when the number of fins is lower. When the number of fins increases, the static pressure rises and the corresponding η is greater because the resistance also increases.
- e. Under the same flow, the higher the rotation velocity, the higher the head height is. Under the same pressure, the higher the rotation velocity, the greater the flow is.
- f. In testing of different rotation velocity, we find that the head coefficient approximates a constant. Under the same lift coefficient, the Q^* of higher rotation velocity is greater than the Q^* of lower rotation velocity.

Nomenclature

- D Equivalent diameter of fan (outer diameter-hub diameter), unit is mm
- dB-A Noise (dB)
- g gravity (m/sec^2)
- H Head height (unit=m)
- I Current (ampere)

- n Rotating speed (rpm)
- P Pressure (N/m²)
- P (%) Fraction of pressure difference
- P* Dimensionless parameter of pressure
- Q volume flow rate
- Q* Dimensionless parameter of volume flow rate
- Q^V Dimensionless value of volume flow rate
- Q_{max}^V Dimensionless maximum value of volume flow rate
- Q (%) Fraction of volume flow rate difference
- Re Reynold's number
- V Voltage (V)
- ρ Air density (1.23kg/m³)
- μ Air dynamic viscosity (1μ=1.8×10⁻⁵ N-sec/m²)
- v air motion viscosity
- η static pressure efficiency

Acknowledgment

The present investigation was supported by National Science Council of Taiwan under granted NSC-97-2221-E-253-014-

References

[1] Suleiman Diary R, Amin Hilmi Fadhil, Husein Nuradin Taha, Using fan speed control method for microprocessors dynamic thermal management, WSEAS Transactions on Circuits and Systems , Vol.5, No.1, 2006, pp. 142-147.

[2] Hur Jin, Sung Ha-Gyeong, Hong Jung-Pyo, . Development of BLDC motor using metal powdered core for 42V fan application of hybrid electric vehicle, WSEAS Transactions on Circuits and Systems, Vol. 4, No. 7, 2005, pp. 812-817.

[3] Muntean Nicolae1, Hedes Alexandru1, Scridon Sever, Babau Radu, Variable speed drive structures and benefits in cooling tower fans

applications, WSEAS Transactions on Systems, Vol. 6, No. 4, 2007, pp. 766-771

[4]Chiang KT., Optimization of the design parameters of Parallel –Plain Fin heat sink module cooling phenomenon based on the Taguchi method, International Communications Heat Mass and Transfer, Vol. 32, 2005, pp.1193-1201.

[5] Fang Q, Shi ZK., Curve fitting method of fan performance map with constraint, Journal of Aerospace Power, Vol. 20, 2005, pp. 630-635.

[6] Wright T., Search for simple models to predict fan performance and noise, Noise Control Engineering Journal, Vol. 43, 1995, pp.85-89.

[7] <http://www.delta.com.tw>.

Table 1. Polynomial coefficient of fitting curves T(x) of different fans.

	AFB606020	AFB505015	AFB606038
a ₀	32.544	13.8480	33.296
a ₁	-3.0369	-6.8475	10.886
a ₂	25.079	98.682	-420.33
a ₃	-76.702	-604.77	5452.9
a ₄	38.847	1798	-33310
a ₅	0	-2852.2	109700
a ₆	0	2262.8	-206920
a ₇	0	-702.72	222940
a ₈	0	0	-127340
a ₉	0	0	29862

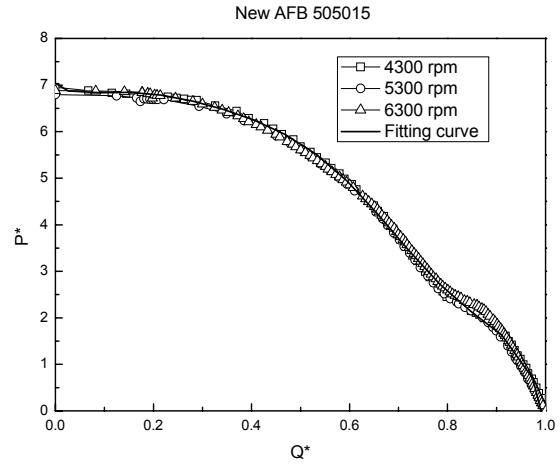
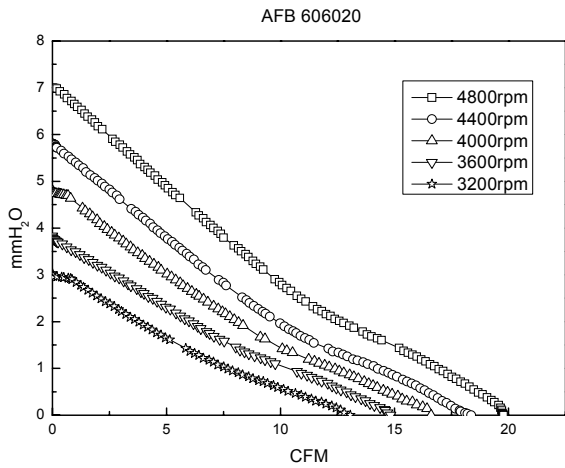
Table 2. Operating point values of conventional approach and dimensionless approach.

Operating point of conventional approach (1)	Operating point of dimensionless approach

	P_1 (mmH ₂ O)	Q_1 (CFM)	P^*	Q^*
4800rpm	2.421	12.320	5.728	0.826
4400rpm	1.857	10.670	6.114	0.812
4000rpm	1.654	9.786	6.472	0.795
3600rpm	1.276	8.869	7.240	0.776
3000rpm	0.980	7.726	7.862	0.755

Table 3. Operating point error of conventional approach and dimensionless approach.

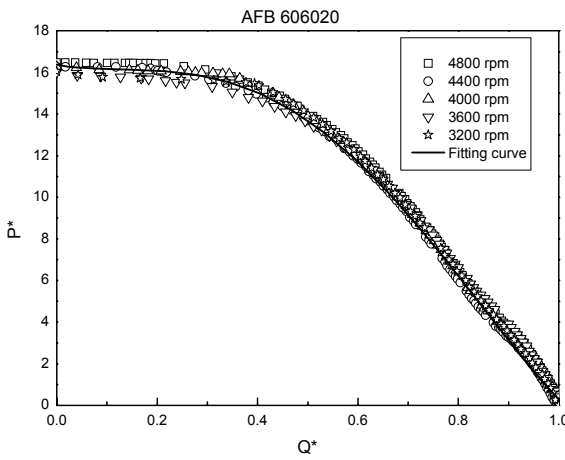
Operating point (P^*, Q^*) and Conversion Unit(P_2, Q_2) of Dimensionless approach---(2) (1) and (2) error ratio				
	P_2 (mmH ₂ O)	Q_2 (CFM)	P(%)	Q(%)
4800rpm	2.54	12.837	4.91%	4.19%
4400rpm	1.951	11.125	4.95%	4.32%
4000rpm	1.735	10.215	4.91%	4.42%
3600rpm	1.335	9.250	4.61%	4.33%
3200rpm	1.030	8.052	4.97%	4.34%



(a)

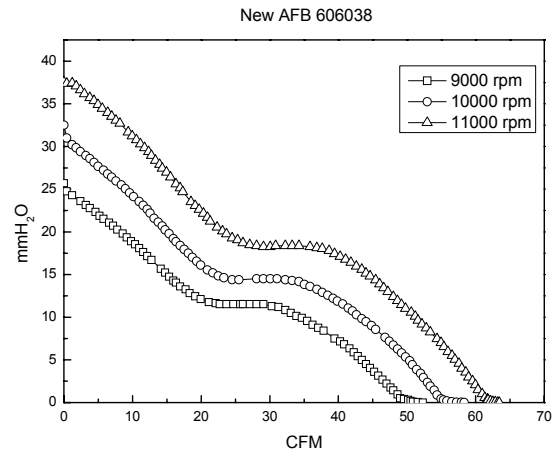
(b)

Fig. 2 Performance curve and fitting curve of New AFB 505015 fan.

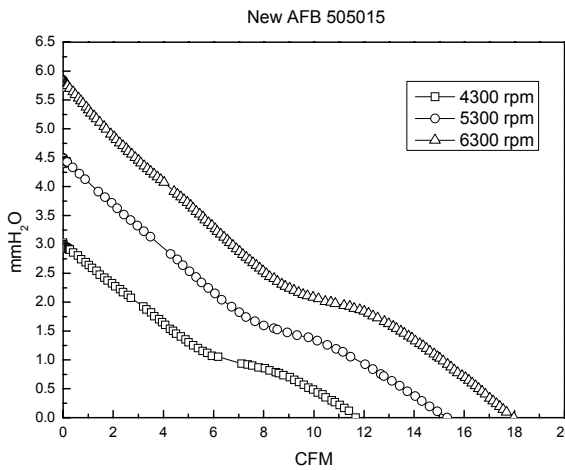


(b)

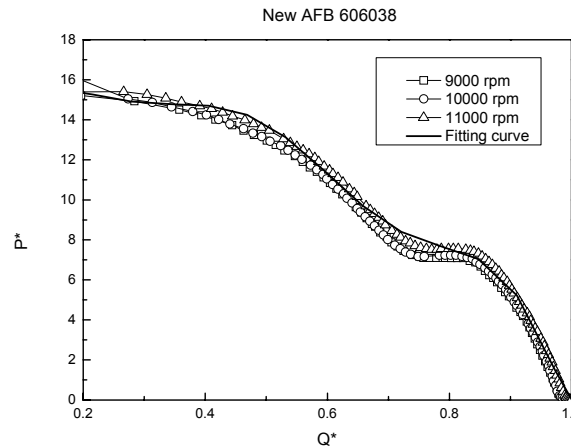
Fig. 1 Performance curve and fitting curve of AFB 606020 fan.



(a)



(a)



(b)

Fig. 3. Performance curve and fitting curve of AFB606038 fan.

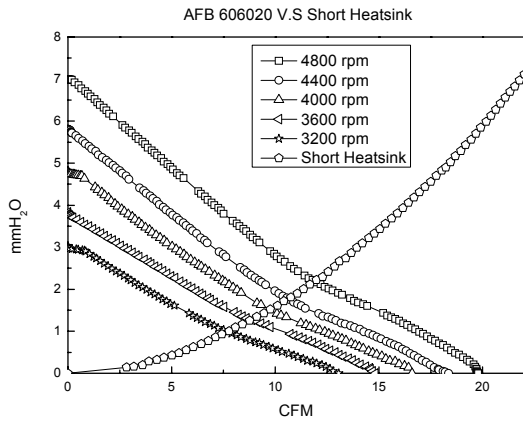


Fig. 4 Impedance curves of different rotating speeds of AFB606020 fan in conjunction with heat sink.

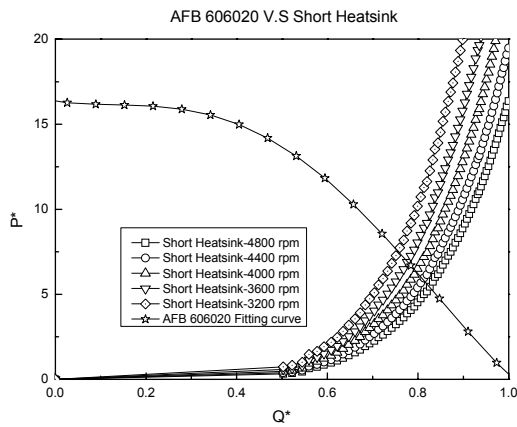


Fig. 5 Dimensionless data of impedance curves of different rotating speeds of AFB 606020 fan in conjunction with heat sink.

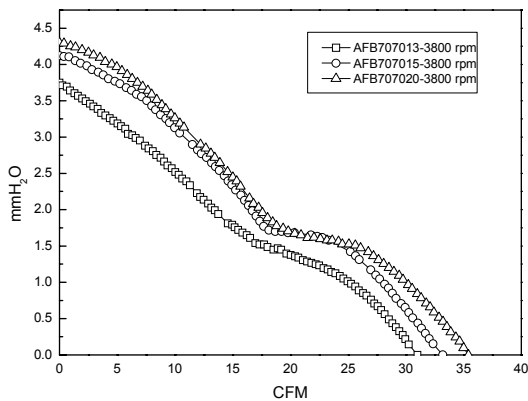


Fig. 6 Effect of different fan thickness on flow and static pressure.

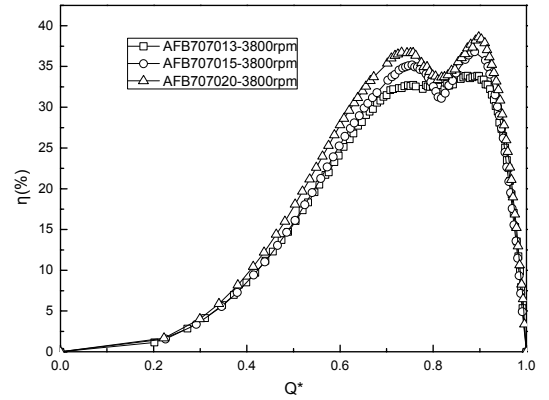


Fig. 7 Effect of different fan thickness on dimensionless flow and static pressure efficiency.

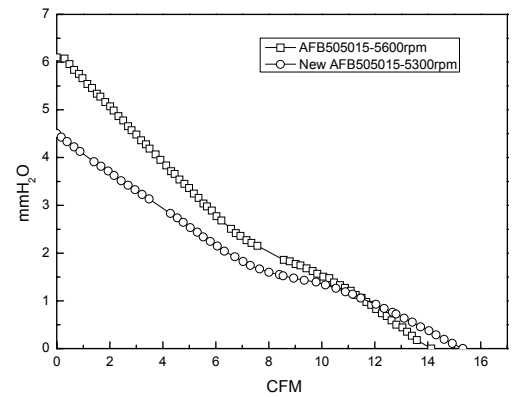


Fig. 8 Effect of different hub ratio on flow and static pressure.

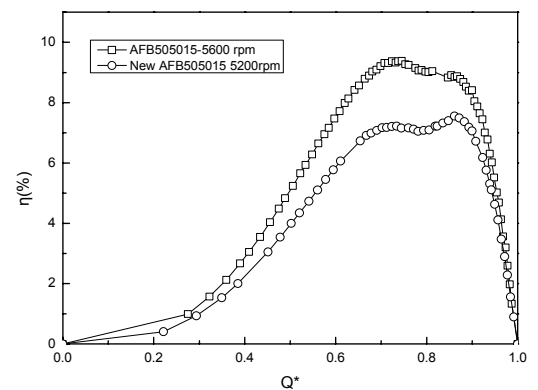


Fig. 9 Effect of different hub ratio on dimensionless flow and static pressure efficiency.

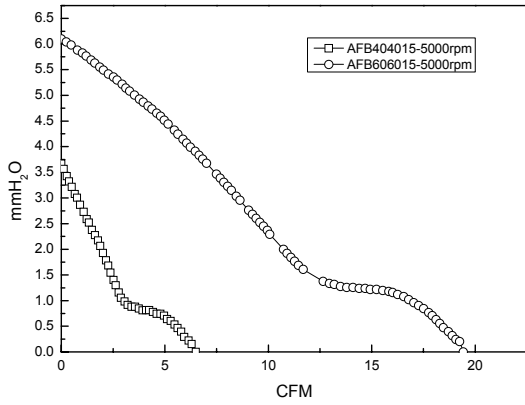


Fig. 10 Effect of fan length and width on flow and static pressure.

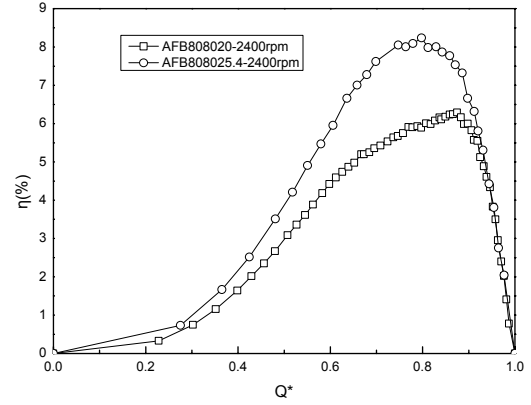


Fig. 13 Effect of different number of fins and thickness on dimensionless flow and static pressure efficiency.

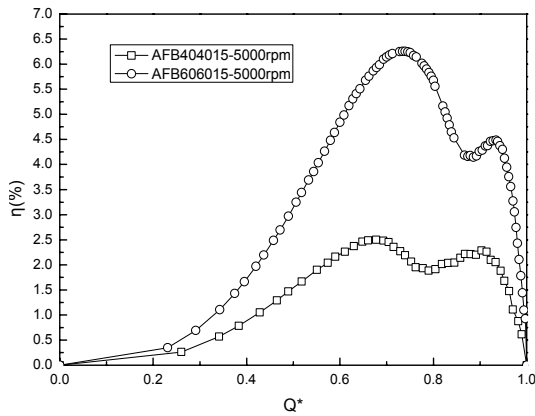


Fig. 11 Effect of different fan length and width on dimensionless flow and static pressure efficiency.

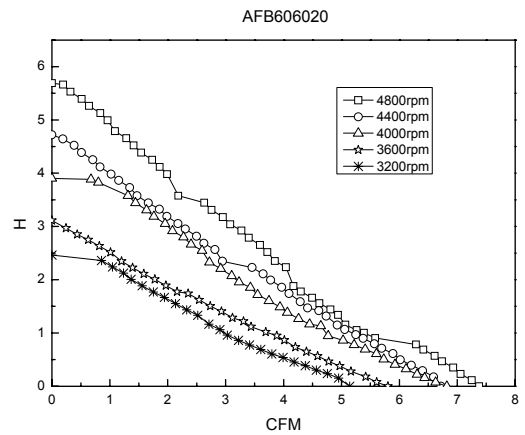


Fig. 14 Effect of different rotation velocity on head height and flow.

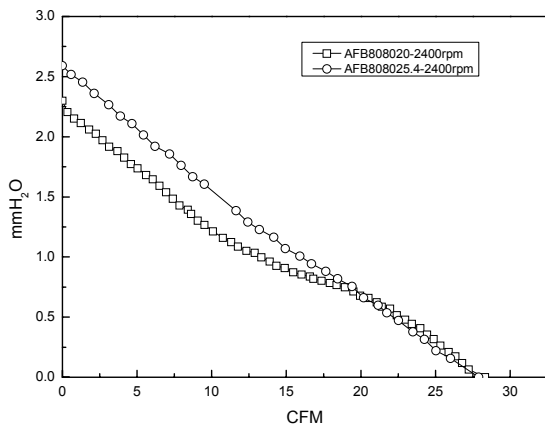


Fig. 12 Effect of different number of fins and thickness on flow and static pressure.

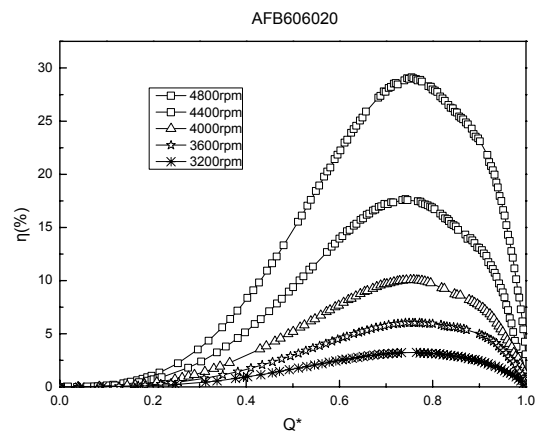


Fig. 15 Effect of different rotation velocity on static pressure efficiency and dimensionless flow.